

Attribution 2.0 Generic (CC BY 2.0)

<https://creativecommons.org/licenses/by/2.0/>

Access to this work was provided by the University of Maryland, Baltimore County (UMBC) ScholarWorks@UMBC digital repository on the Maryland Shared Open Access (MD-SOAR) platform.

**Please provide feedback**

Please support the ScholarWorks@UMBC repository by emailing [scholarworks-group@umbc.edu](mailto:scholarworks-group@umbc.edu) and telling us what having access to this work means to you and why it's important to you. Thank you.

## Accretion geometry in the persistent Be/X-ray binary RX J0440.9+4431

C. Ferrigno<sup>1,a</sup>, R. Farinelli<sup>1,2</sup>, E. Bozzo<sup>1</sup>, K. Pottschmidt<sup>3,4</sup>, D. Klochkov<sup>5</sup>, and P. Kretschmar<sup>6</sup>

<sup>1</sup>ISDC, department of astronomy, Université de Genève, chemin d'Écogia, 16, CH-1290 Versoix, Switzerland

<sup>2</sup>Dipartimento di Fisica Università di Ferrara via Saragat 1, I-44100, Ferrara, Italia

<sup>3</sup>CRESST & University of Maryland Baltimore County, 1000 Hilltop Circle, Baltimore, MD 21250, USA

<sup>4</sup>NASA Goddard Space Flight Center, Astrophysics Science Division, Code 661, Greenbelt, MD 20771, USA

<sup>5</sup>IAAT, Abt. Astronomie, Universität Tübingen, Sand 1, D-72076 Tübingen, Germany

<sup>6</sup>ESAC, ISOC, Villañueva de la Cañada, Madrid, Spain

**Abstract.** The persistent Be/X-ray binary RX J0440.9+4431 flared in 2010 and 2011 and has been followed by various X-ray facilities (*Swift*, *RXTE*, *XMM-Newton*, and *INTEGRAL*). We studied the source timing and spectral properties as a function of its X-ray luminosity to investigate the transition from normal to flaring activity. The source spectrum can always be described by a bulk-motion Comptonization model of black body seed photons attenuated by a moderate photoelectric absorption. At the highest luminosity, we measured a curvature of the spectrum, which we attribute to a significant contribution of the radiation pressure in the accretion process. This allows us to estimate that the transition from a bulk-motion-dominated flow to a radiatively dominated one happens at a luminosity of  $\sim 2 \times 10^{36} \text{ erg s}^{-1}$ . The luminosity dependency of the size of the black body emission region is found to be  $r_{\text{BB}} \propto L_X^{0.39 \pm 0.02}$ . This suggests that either matter accreting onto the neutron star hosted in RX J0440.9+4431 penetrates through closed magnetic field lines at the border of the compact object magnetosphere or that the size of the black-body emitting hotspot is larger than the footprint of the accretion column. This phenomenon can be due to illumination of the surface by a growing column or by a structure of the neutron star magnetic field more complicated than a simple dipole at least close to the surface.

## 1 Introduction

LS V +44 17/RX J0440.9+4431 was classified as one of the rare persistent neutron star Be/X-ray binaries based on the outcomes of the first dedicated *RXTE* monitoring campaign [1], which evidenced a pulsed emission with a period of 202 s. The source distance was later estimated at  $(\sim 3.3 \pm 0.5) \text{ kpc}$  [2]. RX J0440.9+4431 is also reported in the seven-year and nine-year *INTEGRAL* all-sky survey [3, 4]. From the former to the latter catalog, the average flux of the source increased from  $(0.95 \pm 0.15) \text{ mCrab}$  to  $(4.0 \pm 0.1) \text{ mCrab}^1$  (17–60 keV) as it underwent several episodes of enhanced X-ray activity in 2010 and 2011.

<sup>a</sup>e-mail: carlo.ferrigno@unige.ch

<sup>1</sup>In the energy band 17–60 keV these correspond to  $1.35$  and  $5.7 \times 10^{-11} \text{ erg cm}^{-2} \text{ s}^{-1}$ , respectively.

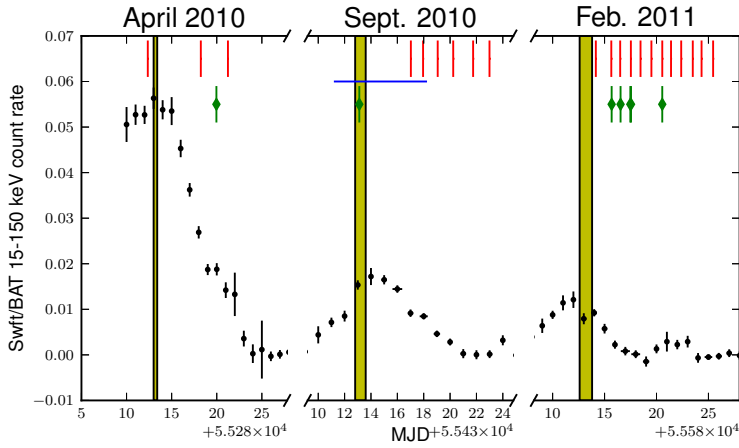


**Figure 1.** Light curve of RX J0440.9+4431 and times of the observations reported in this paper. Black points with errors: *Swift*/BAT daily averaged light curve. Red vertical bars: times of the *RXTE* observations. Blue horizontal bar: time span of the *INTEGRAL* data used in this paper. Green diamonds: times of the *Swift* observations used in our analysis. The first vertical yellow bar indicates the occurrence of the first maximum in the light curve; the others correspond to the times of the following maxima predicted by the orbital ephemeris. MJD 55 280, 55 430, and 55 580 correspond to 2010, March 25, 2010, August 22, and 2011, January 19, respectively.

The first and brightest observed outburst from RX J0440.9+4431, which we are aware of, was detected on 2010 March 26, and lasted until April 15 [5, 6]. The *Swift*/BAT light curve (Fig. 1) showed that the source reached a peak luminosity of about 200 mCrab (15-150 keV) six days after the onset of the event. It remained in this state for eight days, and then turned off to its persistent luminosity level in about ten days. A second outburst from RX J0440.9+4431 was detected by *INTEGRAL* on 2010 September 1. It reached a peak flux of about 80 mCrab both in soft and hard X-rays and lasted about ten days [7]. The analysis of the combined *Swift*, *INTEGRAL*, and *RXTE* data led to identifying a possible cyclotron absorption feature at  $\sim 30$  keV, suggesting a surface magnetic field of  $B \approx 3 \times 10^{12}$  G for the accreting neutron star hosted in this system. This magnetic field intensity would be compatible with the measured properties of the source broad-band noise in the X-ray domain [8].

The two intense X-ray emission episodes recorded from RX J0440.9+4431 showed the typical properties of the so-called “Type I” outbursts, usually displayed when the neutron star in a Be/X-ray binary approaches the system periastron and interacts with the donor’s equatorial disk. The pulsar decreased its spin over the years reaching a period of 206 s, with a net increase of 4 s in seven years. An orbital period of at  $\sim 150$  d is compatible with the expected value for a Be/X-ray binary system [9] and the recurrence of the outbursts. From the *Swift*/BAT light curve of the active phase, it is possible to measure a flux modulation with a period of  $(150.0 \pm 0.2)$  days and the typical profile of the class of objects [10].

Here, we report on the outcome of the monitoring observations of RX J0440.9+4431 during its active phase from the spectral point of view. The large luminosity range of the source and the high throughput of *PCA* allowed us to follow the onset of the X-ray activity starting from the quiescent level with unprecedented accuracy and compare data with theoretical expectations.

## 2 Results

For the data reduction, we have followed standard procedures and used the most updated software and calibration at the time of writing (for the technical details of data analysis, we refer to [10]). Here, we summarise our results on spectral analysis, which are of interest for the interaction of the NS magnetosphere with the surrounding plasma.

### 2.1 Broad-band spectral analysis

The availability of quasi-simultaneous *INTEGRAL*, *RXTE*, and *Swift* data permitted to investigate the broad-band spectral properties of RX J0440.9+4431 (note that part of the data were already presented [8, 11]). First, we have analysed the same data-set of [8] using a spectral model comprising a cut-off power law and a black body component, which could fit the data reasonably well ( $\chi^2/\text{d.o.f.}=1.09/558$ ). As they reported, some residuals are present at  $\gtrsim 30$  keV. However, we found that an additional Lorentzian absorption feature with  $\sigma=6$  keV at  $\sim 30$  keV, as proposed by these authors, did not significantly improve the fit ( $\chi^2/\text{d.o.f.}=1.05/556$ , 33% chance improvement probability). Using on the same data and model we cannot confirm their claim of a cyclotron scattering feature, this can be due to the significant updates in the algorithm of data reduction that we employed.

A better description of the spectrum could be obtained by using the general Comptonization model *BMC* [12] with an exponential cutoff at high energy ( $\text{BMC} \times \exp(-E/E_{\text{Fold}})$ ,  $\chi^2/\text{d.o.f.}=0.92/559$ ), as it can be appreciated in Fig. 2. Because of the general shape of the convolutional kernel, this model can be applied to Comptonization spectra of both optically thin and optically thick regimes, and considering the cases in which thermal or thermal plus bulk Comptonization dominate [13]. From the normalization of the model, it is possible to infer the effective radius of the region in which the seed black body radiation is generated as  $r_{\text{BB,km}} = \sqrt{844 N_{\text{BMC}}/C(kT)_{\text{keV}}^4}$ , where  $C=1$  for a spherical geometry and  $C=0.25$  for a circular slab and we have assumed for RX J0440.9+4431 a distance of 3.3 kpc.

We have tested this model on the *Swift/XRT* and *RXTE/PCA* observations performed in April 2010. At this epoch, the source was brighter, *PCA* data could be used from 3 to 45 keV and an iron line was needed to fit the data (we modeled this as a thin additional Gaussian component centered at  $\sim 6.4$  keV; [11]). Again, no evidence was found for the Lorentzian shaped absorption feature previously reported and we conclude that it is not present in the data.

### 2.2 Spectral variability

To study possible changes in the spectral parameters of the source at different luminosity states, we fit all the available *RXTE/PCA* data, which provided an unbiased monitoring of the source across all different states, by assuming the continuum model discussed in Sect 2.1. The lower energy threshold of the *RXTE/PCA* is 3 keV and it does not permit a precise measurement of the absorption column density in the direction of RX J0440.9+4431. Thus, we have fixed it to the weighted average value measured from all the available *Swift/XRT* and *RXTE* quasi-simultaneous observations ( $N_{\text{H}} = (2.8 \pm 0.1) \times 10^{21} \text{ cm}^{-2}$ ). In several fits the value of  $\log_{10}(A)$ , which quantifies the amount of radiation reprocessed by the Compton kernel in the *BMC* model, could only be poorly constrained. When possible, we estimated a lower limit at 90% c.l., for the lower statistic spectra we fixed it to  $\log_{10}(A) = 1.5$ . During the observations performed when the source reached the highest flux an exponential cut-off at high energy (i.e.,  $\exp(-E/E_{\text{Fold}})$ ) was needed to properly fit the data: we have found  $E_{\text{Fold}} = (30 \pm 6) \text{ keV}$  and  $(33 \pm 8) \text{ keV}$ , respectively. The results obtained from all the fits are reported

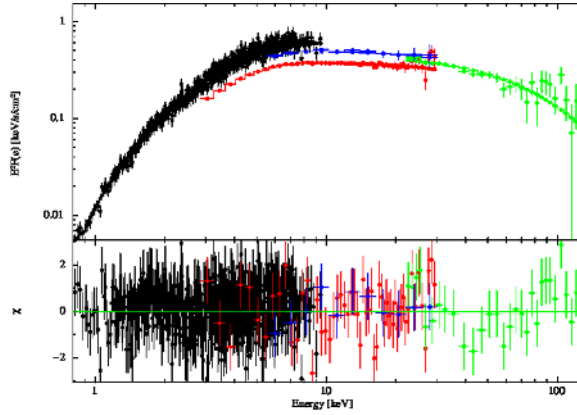


**Figure 2.** Broad-band spectrum of the quasi-simultaneous *INTEGRAL*/ISGRI (green), *INTEGRAL*/JEM-X2 (blue), *RXTE*/PCA (red), and *Swift*/XRT (black) observations performed in September 2010. The best fit is obtained with the absorbed BMC with exponential cut-off model. The residuals from this fit are also shown in the bottom panel.

in Fig. 3. We include in the figure also the EPIC-pn data from the *XMM-Newton* observation that caught RX J0440.9+4431 in its persistent low state [14] for which the BMC model also provided a fully acceptable ( $\chi^2/\text{d.o.f.}=1.1/183$ ).

From the plots in Fig. 3, we note that the parameter  $\log_{10}(A)$  could be only poorly constrained and  $\alpha$  shows a not very pronounced downwards trend for increasing source flux. Conversely, both the effective radius and temperature of the thermal emission component increase with the source flux. For the effective radius, we find ( $\chi^2_{\text{red}}/\text{d.o.f.}=0.6/19$ ):

$$\log_{10} r_{\text{BB}} = (0.182 \pm 0.008) + (0.39 \pm 0.02) (\log_{10} F_{-9}) , \quad (1)$$

where uncertainties are given at  $1\sigma$  c.l.,  $r_{\text{BB}}$  is the effective radius of the black body seed photons expressed in km and  $F_{-9}$  is the 2–30 keV flux expressed in units of  $10^{-9} \text{erg cm}^{-2} \text{s}^{-1}$ . This relation is equivalent to  $r_{\text{BB}} \propto F_X^{0.39 \pm 0.02}$  or  $F_X \propto r_{\text{BB}}^{2.56 \pm 0.13}$ . A similar relation applies to the BB temperature ( $\chi^2_{\text{red}}/\text{d.o.f.}=0.6/19$ ):

$$\log_{10} kT_{\text{keV}} = (0.128 \pm 0.004) + (0.070 \pm 0.008) (\log_{10} F_{-9}) , \quad (2)$$

where  $kT_{\text{keV}}$  is the black body temperature expressed in keV.

### 3 Discussion and Summary

Among different spectral models to account for Compton scattering, the BMC is able to provide a self-consistent and robust physical description of the accretion process in RX J0440.9+4431 over the different luminosity levels, even exploiting a limited energy band.

The *RXTE* observations of RX J0440.9+4431 in 2010 and 2011 allowed us to study spectral changes in the X-ray emission from the source over two orders of magnitude in X-ray flux and mass accretion rates ( $\sim 10^{14-16} \text{g s}^{-1}$ ). The spectra of the lower persistent state are rather soft, they become harder at intermediate states, and display a more pronounced curvature at the highest

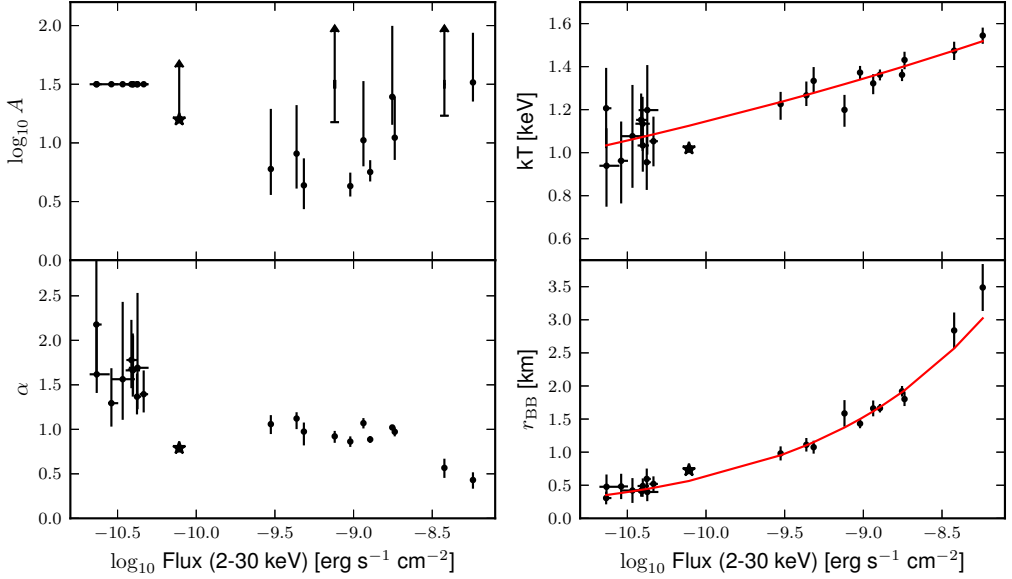


**Figure 3.** Results of the spectral fits to the *RXTE/PCA* observations (filled circles) performed during the outbursts of RX J0440.9+4431 occurred in 2010 and 2011. The best fit spectral parameters obtained from the *XMM-Newton* observation (2011 March 18) are also included and represented with a star (uncertainties are at 68% c.l. and lower limits at 90% c.l.). The BMC model was used for all fits; during the two observations performed when the source reached the highest flux, we introduced an exponential cut-off at high energy. The black body radius  $r_{\text{BB}}$  is obtained setting  $C = 1$ . The red solid lines in the right panels represents the best fit relations obtained from the *PCA* data only.

luminosities. This is in agreement with the measurement of a high-energy exponential cut-off at  $\sim 30$  keV in the *RXTE/PCA* data during the two observations performed when the source flux was  $\geq 10^{-9} \text{ erg cm}^{-2} \text{ s}^{-1}$ .

According to the discussion in [15], at low luminosity ( $L_X \lesssim 10^{34-35} \text{ erg s}^{-1}$ ) matter strikes the NS surface after passing through a gas-mediated shock. At higher luminosity, the radiation pressure begins to affect the accretion process so that a radiative shock forms, and plasma deceleration takes place through Coulomb interactions in an vertically extended atmosphere. At this stage, the efficiency of the thermal cooling of the high-energy electrons responsible for the Comptonized emission increases significantly and can produce the observed change in the cut-off energy. However, the luminosity level at which this transition happens is not well predicted on theoretical basis and is here tentatively identified on observational grounds at  $\sim 2 \times 10^{36} \text{ erg s}^{-1}$ .

Throughout the whole luminosity range, the variation of the parameters of the thermal emission component in RX J0440.9+4431 could be satisfactorily described by the relations:  $r_{\text{BB}} \propto F_X^{0.39 \pm 0.02}$ ,  $kT_{\text{BB}} \propto F_X^{0.070 \pm 0.008}$  (see Sect. 2.1 and Fig 3). In the case of accretion onto a neutron star from the stellar wind, it is expected that the radius of the hot spot is inversely correlated to the luminosity, as at higher accretion rate matter should penetrate along magnetic field lines which are more and more

concentrated towards the NS magnetic poles [16]. Conversely, if the transfer of matter is mediated by an accretion disk, the radius of the hot spot is linked to the X-ray luminosity:  $R_{\text{BB}} \propto L_X^{1/7 \approx 0.14}$  [see, e.g., 17, 18]. The correlation determined from the fits to the data thus support the idea that RX J0440.9+4431 is continuously accreting from a surrounding disk (despite the opposite would be expected for the persistent activity of a Be/X-ray binary). However, the measured relation between  $r_{\text{BB}}$  and the source luminosity is much steeper than expected in the case of disk accretion. This might indicate either that matter penetrates through closed magnetic field lines at the border of the magnetosphere or that the neutron star magnetic field structure is not a simple dipole, at least close to the surface. The former idea was suggested to justify the magnetospheric instabilities observed in the outbursts of EXO 2030+375 [19] and A 0535+262 [20]. The latter has been invoked, e.g., in [21] to interpret the soft component in the broad-band spectrum of 4U 0115+63 and can be related also to accretion-induced deformations of the magnetic field and instabilities in the accretion mound which are shown to exist on the base of recent numerical simulations [22].

Another option is that the increased mass accretion rate produces a significant vertical growth of the accretion column and downward beamed radiation illuminates an annulus around the base of the column. As a consequence, the area of BB emitting surface increases more than the area of the accretion column's footprint. However, we note that there is not a strong signature of a direct BB emission, as it could be expected if the NS is illuminated significantly outside of the accretion stream. Moreover, the area of the external surface of the column is proportional to the total irradiated flux and therefore the height should have a very steep dependency on luminosity if its radius is proportional to  $L_X^{1/7}$ , whereas we find indications of a transition to a radiation dominated flow and thus for a column forming up only at the highest edge of the RX J0440.9+4431's luminosity range.

The way in which the accreting matter penetrates the NS magnetosphere and accretes onto the compact star surface is also producing significant changes in its spin period. We note that RX J0440.9+4431 showed a remarkable spin-down over the past 12 years from 202 s [1] to  $\approx 206$  s [10]. If we assume that RX J0440.9+4431 is accreting from a disk at a non negligible rate, then the measured spin down can be interpreted in terms of coupling between the neutron star magnetic field lines and the external regions of the accretion disk located beyond the so-called corotational radius [23, 24]. This assumption has been sometimes used to constrain the NS magnetic field. As pointed out in [25], the uncertainties on the location and the extension of the boundary layer in the disk accretion models for magnetized neutron stars are relatively large. Therefore, we derive that the magnetic field for the NS in RX J0440.9+4431 is of the order of  $\text{few} \times 10^{12}$  G. This is in agreement with the timing signatures of the broad-band noise [8]. The non-detection of the previously reported cyclotron scattering absorption line discussed in Sect. 2.1 is not a counter argument to this magnetic field estimate, as these features are not ubiquitous in the spectra of accreting magnetized neutron stars.

## References

- [1] P. Reig, P. Roche, *MNRAS* **306**, 100 (1999), arXiv:astro-ph/9902221
- [2] P. Reig, I. Negueruela, J. Fabregat, R. Chato, M.J. Coe, *A&A* **440**, 1079 (2005), arXiv:astro-ph/0506230
- [3] R. Krivonos, S. Tsygankov, M. Revnivtsev, S. Grebenev, E. Churazov, R. Sunyaev, *A&A* **523**, A61 (2010), 1006.4437
- [4] R. Krivonos, S. Tsygankov, A. Lutovinov, M. Revnivtsev, E. Churazov, R. Sunyaev, *A&A* **545**, A27 (2012), 1205.3941
- [5] M. Morii, N. Kawai, K. Sugimori, S. Nakahira, A. Yoshida, K. Yamaoka, M. Sugizaki, T. Mihara, M. Kohama, Y.E. Nakagawa et al., *The Astronomer's Telegram* **2527**, 1 (2010)

- [6] M.H. Finger, A. Camero-Arranz, The Astronomer's Telegram **2537**, 1 (2010)
- [7] R. Krivonos, S. Tsygankov, A. Lutovinov, M. Turler, E. Bozzo, The Astronomer's Telegram **2828**, 1 (2010)
- [8] S.S. Tsygankov, R.A. Krivonos, A.A. Lutovinov, *MNRAS* **421**, 2407 (2012), 1201.0616
- [9] P. Reig, *Ap&SS* **332**, 1 (2011), 1101.5036
- [10] C. Ferrigno, R. Farinelli, E. Bozzo, K. Pottschmidt, D. Klochkov, P. Kretschmar, *A&A* **553**, A103 (2013), 1303.7087
- [11] R. Usui, M. Morii, N. Kawai, T. Yamamoto, T. Mihara, M. Sugizaki, M. Matsuoka, K. Hiroi, M. Ishikawa, N. Isobe et al., *PASJ* **64**, 79 (2012), 1201.6491
- [12] L. Titarchuk, A. Mastichiadis, N.D. Kylafis, *ApJ* **487**, 834 (1997), arXiv:astro-ph/9702092
- [13] R. Farinelli, L. Amati, N. Shaposhnikov, F. Frontera, N. Masetti, E. Palazzi, R. Landi, C. Lombardi, M. Orlandini, C. Brocksopp, *MNRAS* **428**, 3295 (2013), 1211.1270
- [14] N. La Palombara, L. Sidoli, P. Esposito, A. Tiengo, S. Mereghetti, *A&A* **539**, A82 (2012), 1112.5341
- [15] P.A. Becker, D. Klochkov, G. Schönherr, O. Nishimura, C. Ferrigno, I. Caballero, P. Kretschmar, M.T. Wolff, J. Wilms, R. Staubert, *A&A* **544**, A123 (2012), 1205.5316
- [16] J. Arons, S.M. Lea, *ApJ* **235**, 1016 (1980)
- [17] F.K. Lamb, C.J. Pethick, D. Pines, *Astrophysical Journal* **184**, 271 (1973), a&AA ID. AAA010.142.027
- [18] N.E. White, J.H. Swank, S.S. Holt, *ApJ* **270**, 711 (1983)
- [19] D. Klochkov, R. Staubert, A. Santangelo, R.E. Rothschild, C. Ferrigno, *A&A* **532**, A126+ (2011), 1107.2202
- [20] K. Postnov, R. Staubert, A. Santangelo, D. Klochkov, P. Kretschmar, I. Caballero, *A&A* **480**, L21 (2008), 0801.3165
- [21] C. Ferrigno, P.A. Becker, A. Segreto, T. Mineo, A. Santangelo, *A&A* **498**, 825 (2009), 0902.4392
- [22] D. Mukherjee, D. Bhattacharya, A. Mignone, *MNRAS* **430**, 1976 (2013), 1212.3897
- [23] Y.M. Wang, *ApJ* **449**, L153 (1995)
- [24] Y.M. Wang, *ApJ* **465**, L111 (1996)
- [25] E. Bozzo, L. Stella, M. Vietri, P. Ghosh, *A&A* **493**, 809 (2009), 0811.0049



